IDENTIFICATION AND CHARACTERIZATION OF A LARGE SOURCE OF PRIMARY MESENCHYMAL STEM CELLS TIGHTLY ADHERED TO BONE SURFACES OF HUMAN VERTEBRAL BODY MARROW CAVITIES

Brian H. Johnstone, PhD[1,2*], Hannah M. Miller, MS[1,2], Madelyn R. Beck, BS[3], Dongsheng Gu, MD, PhD[1,3], Sreedhar Thirumala, PhD[4], Michael LaFontaine, PhD[2], Gerald Brandacher, MD[5], Erik J. Woods, PhD[1,2,4*]

[1]Ossium Health, Inc. 5754 W. 74th St., Indianapolis, IN 46278

[2]Department of Biomedical Sciences, College of Osteopathic Medicine, Marian University, Indianapolis, IN, USA

[3]Wells Center for Pediatric Research, Indiana University School of Medicine, Indianapolis, IN, USA

[4]Department of Medical and Molecular Genetics, Indiana University School of Medicine, Indianapolis, IN, USA

[5]Department of Plastic and Reconstructive Surgery, Johns Hopkins University School of Medicine, Baltimore, MD, USA

*Address correspondence to: Brian H. Johnstone, PhD or Erik J. Woods, PhD, HCLD(ABB), Ossium Health, Inc., 5754 W. 74th St., Indianapolis, IN, 46278, USA. Email: brian.johnstone@ossiumhealth.com; erik@ossiumhealth.com

ABSTRACT

Therapeutic allogeneic mesenchymal stem/stromal cells (MSC) are currently in clinical trials for evaluating their effectiveness in treating many different disease indications. Eventual commercialization for broad distribution will require further improvements in manufacturing processes to economically manufacture MSC at sufficient scales required to satisfy projected demands. A key contributor to the present high cost of goods (COG) for MSC manufacturing is the need to create master cell banks (MCBs) from multiple donors, which leads to variability in large-scale manufacturing runs. Therefore, the availability of large single donor depots of primary MSC would greatly benefit the cell therapy market by reducing costs associated with manufacturing.

We have discovered that an abundant population of cells possessing all the hallmarks of MSC is tightly associated with the vertebral body (VB) bone matrix and are only liberated by proteolytic digestion. Here we demonstrate that these vertebral bone-adherent (vBA) MSC possess all the International Society of Cell and Gene Therapy (ISCT)-defined characteristics (e.g., plastic adherence, surface marker expression, and trilineage differentiation) of MSC and, therefore, have termed them vBA-MSC, to distinguish this population from loosely associated MSC recovered through aspiration or rinsing of the bone marrow (BM) compartment.

Pilot banking and expansion was performed with vBA-MSC obtained from 3 deceased donors and it was demonstrated that bank sizes averaging $2.9 \times 10^8 \pm 1.35 \times 10^8$ vBA-MSC at passage one were obtainable from only 5 g of digested VB bone fragments. Each bank of cells demonstrated robust proliferation through a total of 9 passages without significant reduction in population doubling times. The theoretical total cell yield from the entire amount of bone fragments (approximately 300g) from each donor with limited expansion through 4 passages is 100 trillion (1×10^{14}) vBA-MSC, equating to over 10^5 doses at 10×10^6 cells/kg for an average 70 kg recipient. Thus, we have established a novel and plentiful source of MSC which will benefit

the cell therapy market by overcoming manufacturing and regulatory inefficiencies due to donor-to-donor variability.

Key words

Human mesenchymal stromal/stem cells

MSC

Vertebral bodies

Bone marrow

Cellular therapy

Regenerative medicine

Large-scale manufacturing

Abbreviations

BM: bone marrow

BM-MSC: bone marrow-mesenchymal stem/stromal cell

CFU-F: colony forming unit-fibroblast

COG: cost of goods

DD: deceased donor

LD: live donor

MCB: master cell bank

MSC: mesenchymal stem/stromal cells

OPO: Organ Procurement Organization

PDT: population doubling time

TNC: total nucleated cells

WCB: working cell bank

VB: vertebral bodies

vBA-MSC: vertebral bone-adherent-mesenchymal stem/stromal cells

INTRODUCTION

The potent activity as well as high expandability of mesenchymal stem/stromal cells (MSC) has generated considerable interest from commercial entities in developing "off-the-shelf" allogeneic MSC therapeutics derived from a limited number of donors. Development of a cellular therapy based on allogeneic "universal donors" allows for controlled manufacture with careful attention to thoroughly assessing quality (e.g., identity, potency, purity, and safety) of each manufactured lot at significant cost savings compared to manufacturing individual lots of autologous cells from individual donors, such as currently occurs for chimeric antigen receptor (CAR) T cell therapies.

The challenges inherent to manufacturing cellular therapies scale with the size of a manufacturing run. Effective doses of MSC for some indications are as high as 1×10^9 cells per dose, which would require manufacturing 10 trillion (10×10^{12}) cells per year to affordably meet potential demand [1-4]. Even at this level of production, with presumed economies of scale, the cost of goods sold (COGS) per dose of MSC could exceed $100,000 [3]. A significant driver of manufacturing costs, which is amplified proportionately with lot size, is the need to replenish master cell banks (MCB) through isolation of MSC from new donors due to the limited volumes of tissues and fluids that can be safely obtained from healthy volunteers and the limited expansion potential of MSC isolated from each donor [5, 6]. MSC are rare in all tissues, comprising, for instance, ~0.001-0.01% of total nucleated cells (TNC) in BM aspirates [7]. Given that BM aspirates from healthy volunteers are limited for the safety of the donor to 100 ml (50 ml bilaterally from iliac crests), the total yield of fresh, non-passaged MSC is approximately 2×10^4/donor. Expansion to a trillion cells would require seed stocks of 1×10^7 MSC in order to limit cell proliferation to 9 population doublings [8]. This number is in addition to the cells reserved for quality control measurements of the expanded MCB and working cell bank (WCB).

Thus, the number of MSC obtainable from each donor is more than 3 orders of magnitude less than is optimal for the initial stages of expansion.

The need to constantly replenish cell banks by obtaining fresh cells from new donors introduces inconsistencies into the manufacturing process due to the observed variability between MSC derived from different donors otherwise matched for attributes such as age and health status [6, 9, 10]. Donor-to-donor variability and the resulting economic impact on manufacturing costs is substantial. In one study that examined large scale manufacturing of multiple lots of MSC derived from different donors, it was found that cumulative population doublings between 5 different BM donors varied by 1.8-fold during 30 days in culture [9]. The result was a >13 day variation in process time to manufacture a batch of 350 million MSC. Besides the logistical burden to coordinate batch runs, there was a commensurate increased cost of growth medium, which is also a key cost-driver for cell-based therapy manufacturing [1, 3, 8]. Furthermore, the authors found that there was >18% difference in colony forming potential and >50% difference in interleukin 6 expression, adding an additional complication to quality control verification of potency for each batch derived from individual donors. Similarly, a single center experience with clinical manufacture of 68 batches of MSC from BM recovered from 59 human volunteer donors observed population doubling times that varied by over 2-fold (46.8-141 hours), averaging 71.7 hours, yielding final batch numbers of MSC ranging from 1.9×10^7 to 5.43×10^9 (average 5.46×10^8) [10].

Besides imposing a direct economic burden of increasing COG per manufacturing run, there is also a regulatory burden with associated costs resulting from the need to refresh cell banks. The MCB serves as the reserve of starter cultures for all manufacturing runs using cells from a particular donor. The regulatory requirements for quality and safety assessments of the MCB are costly and time consuming [11]. Of the three overarching parameters (i.e., safety, potency and identity) required to assess suitability of a manufactured cell therapy product, potency as it relates to individual donor characteristics, is most problematic due to the changing profile that

occurs with expansion, as described above. This is particularly the case as MSC populations near the limits of expansion and enter into senescence which severely limits their potency [12]. For these reasons, population doubling limit is an important factor for regulatory authorities; albeit, one that is not commonly addressed in filings with FDA [13].

Reducing the economic and regulatory burden of generating multiple MCB lots annually to fulfill the need for large scale manufacturing requires identifying large depots of unmanipulated MSC. Potential solutions could come from abundant tissues harboring MSC that are normally discarded following routine medical procedures or are obtainable post-mortem. Adipose-derived stem/stromal cells (ASC) are obtained from elective procedures that commonly yields liters of tissue and have recently been extensively investigated; however, primarily for autologous uses [14, 15]. Isolation directly from medullary cavity-containing bones obtained through medical procedures or cadavers yields higher percentages of MSC (~0.04%) than are present in aspirates, most likely reflecting lack of peripheral blood contamination [16]. Total nucleated cell counts of ~5x10^9 have been obtained from BM of vertebral bodies (VB) recovered from deceased organ donors, with each VB containing ~2x10^6 MSC, or ~2x10^7 total MSC per typical spinal 9 VB segment recovered [17]. In addition, the ilia, sternum, ribs and heads of long bones are sources of BM from which MSC can be recovered [18-20]. Thus, the VB compartment of BM alone from a typical deceased donor yields >3 orders of magnitude more MSC than can be obtained from a healthy human donor.

In addition to cells obtained by eluting or aspirating BM, another population of MSC is tightly associated with medullary cavity bone structures [21-23]. First identified in rodent long bones, bone-adherent MSC (BA-MSC) have subsequently been isolated from human bone fragments obtained from long bone condyles and vertebrae [24]. We have discovered another source of MSC, termed vertebral BA-MSC (vBA-MSC), which remain attached to fragments of VB bone after extensive washing to remove BM cells and can only be liberated by digestion with proteases. The frequency and functionality of vBA-MSC is equivalent to that in eluted VB BM-

MSC. Here we present these data and establish a new source of MSC that could be used in

large scale manufacturing processes to produce batches totaling of over a quadrillion cells from

an individual donor; thus, satisfying the most optimistic levels of demand for decades and

overcoming a current impediment to commercial scale production [2, 8].

MATERIALS AND METHODS

Sources of tissues and cells

Vertebrae were recovered from brain-dead organ donors after obtaining informed consent for research use. Each recovered vertebra was assigned a unique identifier. The inclusion criteria for donor selection were brain death, age between 12 and 55 years, non-septicemic, and disease and pathogen free. Live donor aspirated BM from three healthy volunteers was purchased from Lonza (Walkersville, MD). Expanded live donor MSC, cryopreserved at passage 2, were purchased from Lonza. Relevant donor characteristics are presented in Table 1.

Deceased Donor Tissue Procurement and Transport

Previously developed clinical recovery methods [16, 25] combined with subsequent experience in the ongoing VCA transplant immunomodulation clinical trial (ClinicalTrials.gov Identifier: NCT01459107) at Johns Hopkins University formed the basis for the procurement and transport protocols. A streamlined organ procurement agency (OPO) recovery procedure, combined with dedicated kits and centralized training on recovery and shipment procedures were employed. Recovered bones were shipped to Ossium Health (Indianapolis, IN). Vertebral sections were procured by six different OPO partners: Gift of Hope (Itasca, IL); Donor Alliance (Denver, CO); Iowa Donor Network (North Liberty, IA); Mid America Transplant (St. Louis, MO); and Nevada Donor Network (Las Vegas, NV). Bones were recovered by OPO personnel using an osteotome and mallet under an IRB approved protocol from research-consented organ and tissue donors. Recovered bones were wrapped in lap sponges and towels soaked in saline to ensure moisture retention during shipment. Wrapped specimens were shipped overnight on wet ice to Ossium's processing facility.

Manual Debriding

Upon receipt, in a Biological Safety Cabinet, soft tissue was manually debrided using scalpels and gouges. Once visible, the pedicles were removed using a Stryker System 6 Saw (Stryker, Kalamazoo, MI) leaving only the connected vertebral bodies. Vertebral bodies were separated, and intervertebral disc and soft tissue were removed with a scalpel. Care was taken to ensure that the cortical bone was not breached to preserve and protect the hypoxic cancellous bone marrow throughout the entire debriding process.

Using custom-made surgical grade stainless-steel anvil shears, VBs were cut into approximately 5 cm^3 pieces small enough to be fragmented with a bone grinder. The pieces were immediately submerged into 500 mL processing medium comprised of Plasma-Lyte A pH 7.4 (Baxter Healthcare, Deerfield, IL), containing 2.5% human serum albumin (HSA; Octapharma USA Inc., Hoboken, NJ), 3 U/ml Benzonase (EMD Millipore, Burlington, MA), and 10 U/ml heparin (McKesson, Irving, TX).

Grinding and Elution

A bone grinder (Biorep Technologies. Inc, Miami, FL) was assembled in a biological safety cabinet. A two-liter stainless steel beaker containing approximately 250 mL of fresh processing medium was placed under the grinding head to catch bone chips and media flow-through. A stainless steel plunger was used to aid in pushing pieces through the grinder. Rinsing through the grinder with processing medium prevented bone pieces from drying out and sticking to the chamber. Once all bone pieces were ground, the chamber was thoroughly rinsed with fresh processing medium. The final volume in the stainless-steel beaker was one liter.

Filtering was performed using bone marrow collection kits with flexible pre-filter and inline filters (Fresenius Kabi, Lake Zurich, IL). All bone grindings and media were carefully transferred to the bone marrow collection kit. The grindings were gently massaged to allow for optimal cell release from grindings. The media was then filtered using two 500 μm and two 200 μm filters. The

bone grindings are rinsed using two 500 mL washings with rinse media. Rinse medium was Plasma-Lyte with 2.5% HSA. All bone marrow was then collected in a collection bag. The bone fragments remaining in the filtration kit were stored at 4°C overnight before processing to recover vBA-MSC.

Digestion protocol for vBA-MSC isolation

Bone fragments (either 1 or 5g) were transferred to sterile 50 ml conical centrifuge tubes. A solution of DE10 collagenase (2 mg/ml; Vitacyte, Indianapolis, IN) was added to the bone fragments at a ratio of 5:1 (volume:weight). The tubes were transferred to a shaking incubator and incubated for 1.5 hrs at 37°C while shaking at 125 rpm. Protease activity was neutralized by adding 2% Stemulate (Cook Regentec, Indianapolis, IN) and suspensions were filtered through a 70 μm cap filter into 50 ml conical screw cap tubes. The filter-retained bone fragments were washed with 25 ml Dulbecco's modified phosphate buffered saline (DPBS) solution containing heparin (10U/ml) and Benzonase (100 U/ml; Millipore, Burlington, MA) which was combined with the original filtrate. Tubes were centrifuged at 350xg for 5 minutes, supernatant aspirated, and the pellets were resuspended in 25 ml DPBS. The suspension was centrifuged again at 350xg for 5 minutes, the supernatant was aspirated, and the pellet was resuspended in 10 ml DPBS for analysis.

Isolation of MSC from iliac and VB BM

An 1 ml aliquot of concentrated, eluted BM was removed and pipetted into a 50 ml conical vial along with 49 ml DPBS. The vial was centrifuged at 300xg for 10 minutes, supernatant aspirated, and the pellet resuspended in 10 ml Rooster-Nourish medium (Rooster Bio, Frederick, MD). Cells were counted and cultured as described below

Cell counting

A Cellometer Vision (Nexcellom, Lawrence, MA) was used to determine total viable cell counts. 20 μl ViaStain AOPI reagent (Nexcelom) was added to an Eppendorf tube containing 20 μl of cells. Once mixed, 20 μl of the solution was added to a Cellometer slide and total cells, live cells, and viability were calculated.

Cell Culture

Fresh cells were plated in CellBIND® T-225 flasks (Corning, Tewksburry, MA) at a density of 25,000 viable cells/cm^2 in RoosterNourish^{TM} medium (Rooster Bio, Frederick, MD). Nonadherent cells were removed after the first media change on day 1. Media was then changed every 3-4 days until colonies were ~80-90% confluent (12-14 days). Cells were released with TrypLE (ThermoFisher Sceintific, Waltham, MA). Passaged cells were plated at a density of 3,000 cells/cm^2 but otherwise followed the same protocol as freshly plated cells.

Generation of MCBs from three donors (DD5, DD6 and DD7) was performed in CellBind® Hyperflasks. Fresh, primary digests were initially plated at 25,000 viable cells/cm^2 as above. Cells were released with TrypLE and expanded one more passage to form the MCB. The bulk of passage 1 cells were resuspended in cryopreservation medium (CryoStor CS10; BioLife Solutions, Bothell, WA) and stored in the vapor phase of liquid nitrogen.

Cells were passaged up to nine times in a medium composed of DMEM (Cat#10567014, ThermoFisher, USA) and pathogen reduced human platelet lysate (nLivenPR^{TM}, COOK Regentec, USA), with and without the addition of ascorbic acid (248 μM; Cat# A2218, Sigma, USA), recombinant basic fibroblast growth factor (10 ng/ml; Cat#233-GMP-025, R&D Systems, USA) and recombinant epidermal growth factor (10 ng/ml; Cat#236-GMP-200, R&D Systems, USA). Cells at 70-80% confluency were harvested and total cell counts were obtained. A portion of the cells was replated at 3000 cells/cm^2 in triplicate wells of a six-well plate, with media changes every 3-4 days.

Phenotypic Analysis of MSC via Flow Cytometry

At passages 2, 3 and 4, 1.8 μl of the following single fluorescently-conjugated antibodies or dye, CD3, CD14, CD19, CD31, CD34, CD45, HLA-DR, CD73, CD90, CD105, Stro-1, and 7AAD (Supplemental Table S1), were added to different wells of a 96-well V-bottom plate. 100 μl of MACS (Miltenyi Biotec, Auburn, CA) buffer and 100 μl of cells (200,000 cells) were added to each well containing an antibody. The plate was incubated at 4°C for 30 minutes shielded from light and afterward, the plate was centrifuged for 5 minutes at 300 x g. Cells were washed and resuspended in 200 μl of MACS buffer. An ACEA Biosciences NovoCyte 2060R flow cytometer was used for data collection and data was analyzed using NovoExpress software (Acea Biosciences San Diego, CA).

Trilineage Differentiation of MSC

MSCs at passages 1 or 3 were seeded in wells of a 12-well plate containing 3 ml Mesencult (Stem Cell Technologies, Vancouver, B.C.) each at $8.0\text{x}10^4$, $4.0\text{x}10^4$, and $2.0\text{x}10^4$ for chondrogenesis, adipogenesis, and osteogenesis differentiation. Wells containing $4.0\text{x}10^4$ MSCs in Mesencult medium served as controls. After incubating for 2 hours, Mesencult in the chondrogenesis well was replaced with StemPro chondrogenesis medium (Thermo Fisher Scientific, Waltham, MA). After one day, Mesencult in the adipogenesis and osteogenesis wells was aspirated and replaced with StemPro adipogenesis medium and StemPro osteogenesis medium, respectively. Respective differentiation media were replenished every 3 days as well as Mesencult in control wells. After 14, 12, and 16 days, wells containing chondrocytes, adipocytes, and osteocytes, respectively, were aspirated of media, washed twice with DPBS, fixed with 4% formalin for 30 minutes, washed once with DPBS, and stained. Alcian Blue, which stains chondrocyte proteoglycans blue, in 0.1 N HCl was added to the chondrocyte wells for 30 minutes, the stain was aspirated, the well was washed three times with 0.1 N HCl and

neutralized with distilled water, and chondrocytes were visualized under an inverted light microscope (Nikon). Oil Red O, which stains adipocyte fat globules red, was added to the adipocyte well for 15 minutes, the stain was aspirated, the well was washed three times with distilled water, and adipocytes were visualized under an inverted light microscope. 2% Alizarin Red, which stains osteocyte calcium deposits red, was added to the osteocyte well for 3 minutes, the stain was aspirated, the well was washed three times with distilled water, and osteocytes were visualized under an inverted light microscope. All differentiated cells were qualitatively analyzed by visualization of color and morphology.

Quantitative RT-PCR analysis of gene expression during differentiation

The RNA was isolated from differentiated cells using TRIzol RNA Isolation reagents (Invitrogen, USA) and cDNA was produced using High-Capacity cDNA Reverse Transcription Kit (Applied Biosystems™, USA). The primers (Supplemental Table S2) were obtained from Integrated DNA Technologies Inc. (USA) and were used to measure the gene expressions of the adipogenesis-related proteins lipoprotein lipase (LPL) and fatty acid binding protein 4 (FABP4), osteogenesis-related proteins osteonectin, osteopontin and collagen type-1, and chondrogenesis-related proteins aggrecan, collagen type-2, and SOX9. The real time PCR assays were run on Bio-Rad C-1000 Touch (Bio-Rad, USA) Real-Time PCR System. The data were analyzed relative to the housekeeping gene, GAPDH, then the fold change of gene in differentiated cells was calculated relative to undifferentiated cells.

Population doubling time

Population doubling time was determined at each passage by using the formula: $t*\log(2)/\log(T_1/T_0)$, where t is the time (hours) between initial plating and cell harvest at 90% confluency, T_1 is the cell count at harvest and T_0 is the initial count at seeding.

CFU-F assays

For freshly digested cells, 5 ml Mesencult, 20 µl Amphotericin B, and 100 µl Gentamycin were added to three wells of a 6-well plate. $2.5x10^5$, $5.0x10^5$, and $7.5x10^5$ cells were added to the first, second, and third wells, respectively. Plates were placed in the incubator until colonies were 90% confluent or up to 12 days. Media was changed every 3-4 days for 14 days. Plates were washed twice with DPBS, and 2 ml methanol was added to each dish for 5 minutes to fix the cells. After 5 minutes, the methanol was decanted, the plate was allowed to air dry and colonies were stained with a 1% crystal violet solution. Colonies containing >50 cells were scored. Passaged cells were assayed similarly except that cells were plated at densities of 32 cells/cm^2, 65 cells/cm^2, and 125 cells/cm^2.

T cell suppression assays

Suppression of T cell activation was performed according to previously published protocols with minor modifications [26]. Briefly, peripheral blood mononuclear cells were isolated from whole blood (10 ml) by Ficoll (GE, Chicago, IL) separation and resuspended in DPBS. The majority of cells were labeled with carboxyflourescein diacetate succinimidyl ester (CFSE; Sigma, St. Louis, MO) and frozen until used [27]. Passage 2 or 3 MSCs, in some cases pre-stimulated with 100 ng/ml interferon-γ (IFNγ; RnD Systems, Minneapolis, MN) for 18-24 hours, were resuspended in Rooster Nourish (RoosterBio, Frederick, MD) and added to a 96 well flat bottom plate at $4x10^5$, $1x10^5$, $5x10^4$, $2.5x10^4$, $1.5x10^4$, $5x10^3$ cells/well. Rooster Nourish was added to each well until the volume was 200 µl/well. The plate was placed in a 37ºC incubator with 10% CO_2 at 5% humidity for at least two hours to allow MSCs to attach. Cryopreserved PBMCs were quickly thawed and resuspended at a concentration of $4x10^6$ cells/ml in Eagle's minimal essential medium (EMEM; Stem Cell Technologies; supplemented with 10% FBS, 100 µg/ml PenStrep, 2 mM L-glutamine, and 100 µM β-mercaptoethanol). The medium was aspirated from the plates containing MSC and 100 µl of PBMCs were added to all wells containing MSCs as well as wells without MSCs. T cells were stimulated by adding 100 µl of supplemented EMEM with 40 µg/ml

phytohemagglutinin (PHA; Sigma-Aldrich, St. Louis, MO) to each well containing MSCs and PBMCs. Control wells containing CSFE-labeled and unlabeled PBMCs alone were also included, half of which were stimulated with PHA and half which were not. The plate was returned to the incubator. After 4 days, PBMCs from each well were removed and labeled with 5 µl CD3-PE and 5 µl of 7AAD before performing flow cytometry

Statistics

GraphPad Prism version 8 was used for statistical analysis (Student's *t* Test). An P value < 0.05 was considered significant.

RESULTS

A typical vertebral column (typically T8-L5) before and after removing soft tissues, separating VBs and then fragmenting to sizes of approximately 1.5 cm^3 is shown in Figure 1. Plastic adherent vBA-MSC possessed a typical spindle-shaped morphology in culture (Figure 1D). Cells from donors were expanded through passage 4 (the initial plating was considered passage 0) and assayed by flow cytometry. vBA-MSC at passages 1-4 expressed very low levels of hematopoietic cell surface markers CD14, CD19, CD34 and CD45 and expressed low to non-existent amounts of human leukocyte antigen DR (HLA-DR) (Figure 2A). The gating strategy and representative flow cytometry dot plots are shown in Supplemental Figure S1. Levels of PECAM1 (CD31)-expressing cells (typically endothelial cells and monocytes) were also low (<7%) at passage 2 (data not shown). Conversely, passaged vBA-MSC were uniformly positive for CD73, CD90 and CD105. Thus, vBA-MSC possess the characteristic MSC surface marker profile [28]. In addition, a variable portion (approximately 20% or lower, depending on the passage number) of the population also expressed the multipotential MSC surface marker Stro-1 [29-32].

Chondrogenic, adipogenic and osteogenic potentials of passage 3 vBA-MSC were determined for each donor. Each of the vBA-MSC isolates demonstrated the potential to differentiate into chrondrocytes, adipocytes and osteocytes as determined by histology (Figure 2B) and quantitation of RNA transcripts associated with each differentiation pathway (Figure 2C). A portion of both freshly isolated (i.e., never plated) as well as passaged vBA-MSC demonstrated high degrees of clonal proliferation, as determined by colony forming unit-fibroblast (CFU-F) potentials. The average CFU-F frequency in freshly digested VB bone fragments was 0.01±0.004% (mean±standard deviation), which is similar to the frequency of proliferative MSC in whole BM (Figure 3) [7]. The proliferative cells were maintained with cell

culture, forming colonies at a frequency of 37$\pm$3.4% and 27$\pm$1.2% after one and two passages, respectively.

Suppression of T cell activation is one of the best studied therapeutic properties of MSC, providing the rationale for testing in clinical trials of inflammatory disorders [33, 34]. vBA-MSC from the three different donors dose-dependently suppressed T cells activation with PHA (Figure 4). Maximum suppression at a 1:1 ratio of vBA-MSC to peripheral blood mononuclear cells (PBMC) was 89$\pm$7%. A slight but non-significant increase in suppression at all ratios was observed by pre-treating vBA-MSC with IFN-γ for 18-24 hours prior to performing the suppression studies. Treatment with IFN-γ has been shown to stimulate immunosuppressive functions of MSC, with enhanced effects on senescent cells [12]. The insensitivity to priming with concentrations of IFN-γ shown previously to stimulate T cell suppression may indicate that vBA-MSC retain full immunomodulatory capacity during culture expansion.

The immunophenotypic profile of plastic adherent vBA-MSC, trilineage differentiation capacity and CFU-F potential as well as immunomodulatory properties confirm the classification of these cells as MSC according to the International Society of Cell and Gene Therapy (ISCT) published guidance [28]. To further establish their equivalency to MSC obtained from BM, a comparison was performed between vBA-MSC and MSC isolated from central BM (Figures 5 and 6). Both commercially available previously expanded live donor BM-MSC (Ex LD BM-MSC), obtained cryopreserved at passage 2, as well as MSC freshly isolated from live donor aspirated BM (LD BM-MSC) were used. In addition, MSC isolated from deceased donor VB BM (DD vBM-MSC) was also included in the comparison. MSC from three donors for each source were expanded to passage 2 and cryopreserved. Upon subsequent thawing, cells were passaged once prior to performing the analyses. MSC from all four sources demonstrated essentially identical immunophenotypic cell surface marker profiles, with very low numbers of cells that

expressed CD14, CD19, CD34, CD45 and HLA-DR, and, conversely, nearly all cells expressed CD73, CD90 and CD105 (Figure 5A).

MSC from each source grew rapidly in culture through 5 passages (the longest period examined) with no differences in population doubling times (PDTs) at passages 4 and 5 (Figure 5C and D). The Ex LD BM-MSC, which were obtained pre-expanded to passage 2, did exhibit significantly higher PDTs at passage 3 than the other thee MSC populations (Figure 5B). The CFU-F potential of passage 2 Ex LD BM-MSC was also significantly lower than the other MSC populations (Figure 5E). Later passages were not compared for CFU-F potential. Finally, trilineage differentiation potentials were compared and it was found that each MSC population formed adipocytes, chondrocytes and osteocytes *in vitro* at qualitatively the same frequencies (Figure 6).

The potential clinical translational utility of vBA-MSC was assessed by performing a pilot-scale manufacturing run to examine feasibility of banking and expanding large numbers of cells from individual donors. Fragments of VB from 3 different donors were digested to isolate vBA-MSC. The amount (5 g) corresponds to approximately 1/60 of the total VB bone fragment weight (300 g) obtainable from typical donors. Cells enzymatically liberated from VB fragments were plated in a DMEM/human platelet lysate base medium with and without the addition of growth factors and ascorbic acid (see Materials and Methods section). The addition of FGF-2 and EGF was required for optimal growth rate and final yields (S. Thirumala, manuscript in preparation), as demonstrated previously [35]. An MCB at passage 1 from each donor, containing an average of $2.9 \times 10^8 \pm 1.35 \times 10^8$ vBA-MSC, was prepared and the bulk cryopreserved, while the remainder was cultured over multiple passages, tracking total cell yields at each passage (Figure 7A). Passage 1 was considered to be optimal for an MCB, displaying essentially the same surface marker profile and CFU-F potential as later passages (Figures 2 and 3). A single further expansion to passage 2 was enough to produce an WCB containing $5.17 \times 10^9 \pm 4.3 \times 10^9$ vBA-

MSC. Based on observed population doublings, two expansions of the entire WCB were sufficient to manufacture over 2×10^{12} (two trillion) cells. The PDT remained nearly constant between passages 2 and 9, without indications of diminishing growth rate at the upper passage number. However, there were differences in PDTs between donors (Figure 7B). Based on the observed PDTs for each donor, starting with a seed stock of 2 million vBA-MSC, it would require 23, 36 and 29 days to manufacture one trillion cells from the three different donors. These times were calculated using 2-dimensional tissue culture flasks and would likely differ in 3-dimensional bioreactors.

DISCUSSION

The transformative potential of MSC to treat a wide variety of medical disorders has been idealized for over a decade; yet, despite many demonstrations of this potential in preclinical and early-stage clinical trials, no MSC-based therapies have achieved success in late-stage, registration (commonly Phase 3 in the U.S.) clinical trials, although a few have received approval for limited indications in relatively small jurisdictions. The reasons for the slow progress in approvals and resulting commercialization of therapeutic MSC despite intense development efforts by multiple entities is certainly multifactorial. In hindsight, it appears that attempts to manufacture MSC at large scale through adopting processes and procedures from the highly successful biopharmaceutical sector might have been a contributory factor [36, 37]. There are many differences between manufacturing products derived from cells versus the cells themselves. Biopharmaceuticals are produced using immortalized cell lines having the ability of nearly unlimited expansion, allowing the generation of large MCBs from a single seed stock. Conversely, the limited availability and expansion potential of MSC requires generating multiple

MCB from different donors each year at a disproportionately higher manufacturing costs and regulatory burden [37].

We present here a viable solution to reducing these burdens through the identification and characterization of a large depot of MSC from deceased donor vertebral bones. Based on the analysis presented here, vBA-MSC are phenotypically and functionally equivalent to MSC obtained from central BM. The cells express typical MSC surface markers (CD73, CD90 and CD105) and lack expression of hematopoietic cell surface markers as well as HLA class II proteins (Figures 2 and 5A). Like BM-MSC, vBA-MSC possess the potential to clonally expand and can be induced to undergo trilineage differentiation (Figures 2, 3, 5 and 6). Passaged vBA-MSC are fully fit to suppress T cell activation, demonstrating no difference in activity with prior stimulation by IFN-γ (Figure 4). The differences in PDT and CFU-F of passage 3 (but not later passages) expanded BM-MSC obtained from a commercial source most likely reflects a slower recovery from cryopreservation at passage 2 (Figure 5B). All MSC were grown to passage 2 and cryopreserved in an effort to maintain comparability; however, the commercial source of expanded BM-MSC were likely grown in a different medium and frozen in a different cryopreservation medium. Thus, the cells experienced a lag upon thaw and growth to passage 3 which was not evident in subsequent passages.

Master cell bank sizes averaging 2.9×10^8 passage 1 vBA-MSC were obtainable from only approximately 1/60th (5 g) of the total digested VB bone fragments recovered from each of 3 donors (Figure 7A). The calculated total yield at passage 4 of vBA-MSC from each donor in this study is over 1×10^{14} (one hundred trillion) cells, equating to over 10^5 doses at 10×10^6/kg for an average 70 kg patient. More recent experience, following further optimization of isolation and expansion protocols, suggests an order of magnitude greater yield at each passage is attainable (Ossium internal data). Inevitably, actual total cell yields will be lower due to inefficiencies inherent in large scale manufacturing and requirements for testing; nonetheless, the COG for

production of large batches of vBA-MSC from a single donor would likely be much less than for equivalent scales of manufacturing of BM-MSC from multiple donors. The savings in direct manufacturing costs would be in addition to the reduced regulatory burden with using a single donor source for all manufacturing campaigns. The next step in validating the potential cost savings with vBA-MSC will be to perform scaled-up manufacturing runs, which are currently in progress.

We are presently exploring the question of why some populations of MSC are easily dislodged or possibly free floating in the BM, while others remain tightly adhered to the bone/connective tissue matrix and can only be liberated by enzymatic digestion. Determining differences, if they exist, is complicated by the relatively low frequency (<0.01%) of these cells, making them problematic to characterize using common analytical tools, such as flow cytometry, without first expanding in culture, which induces phenotypic and functional alterations [38-46]. One previous report found that freshly isolated enzymatic digests of pelvic region trabecular bone contained 15-fold higher CFU-F than aspirated BM [24]; however, we did not find a similar difference between freshly isolated vBA-MSC and BM-MSC. To better understand dissimilarities, if any, between the populations, we are pursuing single cell RNA sequencing (scRNA-Seq) of vBA-MSC transcriptomes [47, 48]. We are also continuing to characterize the therapeutic potential of vBA-MSC by studying the secretome and extracellular vesicles produced by these cells.

This study was restricted to characterizing vBA-MSC from young, healthy donors between the ages of 15 and 31 years. We also have successfully isolated these cells from older donors (up to 56 years) and demonstrated expansion in culture (unpublished data). However, we intentionally focused on young donors in this report given the literature suggesting higher frequencies and proliferation rates of MSC derived from various tissues obtained from young donors compared to their older counterparts [49-55]. Therefore, in the absence of impacts from

environment and disease status, the lowest COG to manufacture vBA-MSC would be from young donors.

In summary, based on the data presented here, the fundamental nature of vBA-MSC does not appear to differ from aspirated BM-MSC; therefore, these cells could potentially be seamlessly substituted for therapeutic applications at a significant savings in manufacturing and regulatory costs. Additionally, other markets requiring large numbers of MSC could also benefit from an abundant source of primary cells. These include tissue engineering and manufacture of products derived from MSC, such as exosomes, as well as biomedical research applications and the emerging applications of cosmeceuticals and bioengineered materials. Each of these markets is expected to grow substantially over the next decades, driving combined demand for MSC in excess of 10 sextillion (1×10^{21}) cells annually by 2040 [2]. Future high demand for MSC across all these markets could be entirely met by vBA-MSC obtained from the abundant and steady supply of deceased donor medullary cavity containing bones from the >10,000 organ donors and a further >40,000 tissue donors each year in the U.S. alone [56].

Acknowlegements

TABLES

Table 1. Description of donors used in this study

Donor ID	Recovered MSC	Age	Sex	Race/ Ethnicity
DD1[1]	vBA-MSC, vBM-MSC	22	M	Caucasian
DD2	vBA-MSC, vBM-MSC	13	M	Caucasian
DD3	vBA-MSC	35	M	Hispanic
DD4	vBA-MSC, vBM-MSC	19	M	Hispanic
DD5	vBA-MSC	17	M	Caucasian
DD6	vBA-MSC	14	M	Caucasian
DD7	vBA-MSC	23	M	Caucasian
LD1	LD BM-MSC	20	F	African American
LD2	LD BM-MSC	23	F	African American
LD3	LD BM-MSC	28	M	African American
LD4	Ex LD BM-MSC	24	F	African American
LD5	Ex LD BM-MSC	36	M	African American
LD6	Ex LD BM-MSC	25	M	African American

[1]Abbreviations: DD, deceased donor; LD, live donor; vBM-MSC, vertebral bone marrow-MSC; vBA-MSC, vertebral bone-adherent MSC,

Figure legends

Figure 1. Processing of a typical vertebral column to isolate vBA-MSC. Vertebrae (typically T8-L5) were cleaned of soft tissue (A) before separating vertebral bodies (VBs) and removing disks and remaining soft tissues (B). VBs are ground to approximately 1.5 cm^3 fragments (C) before enzymatic digestion to release adherent cells. Plastic adherent vBA-MSC form typical spindle shapes in culture (D; passage 2 cells).

Figure 2. Surface antigen phenotype and trilineage differentiation of vBA-MSC. (A) Passage 1, 2, 3 and 4 vBA-MSC from 3 different donors (DD1, DD2 and DD3; Table 1) were analyzed for surface antigen expression using fluorescently-conjugated antibodies and flow cytometry. The percentage of cells (gated on whole cells using side and forward scatter) after culturing for each passage is shown. (B) Passage 3 vBA-MSC grown in expansion medium (B-A) or induced to undergo either (B-B) chondrogenesis, (B-C) adipogenesis or (B-D) osteogenesis were imaged after staining for chrondocytes (alcian blue), adipocytes (oil red O) or osteocytes (alizarin red), as described in Materials and Methods. Images are representative of results with the 3 different donor-derived vBA-MSC. Magnification for all 20X. (C) Quantitation of differentiation by analysis of (a,b) adipogenic (lipoprotein lipase and fatty acid binding protein-4), (c-e) chondrogenic (aggrecan, collagen 1 and SOX9) and (f-h) osteogenic (osteopontin, osteonectin and collagen 1) RNA markers in undifferentiated (Undiff) and differentiated (Diff) vBA-MSC cultures by quantitative RT-PCR. Relative mRNA levels are shown. *, P<0.05, unpaired Student's t-Test comparing undifferentiated to differentiated cells.

Figure 3. Colony forming unit-fibroblast (CFU-F) potential of vBA-MSC isolated from 3 different donors (DD1, DD2 and DD3; Table 1) and plated immediately after isolation by digestion (fresh) or after 1 or 2 passages (P1 and P2). Either 5x10^5 (fresh) or 624 (passaged) total cells from each of 3 donors were plated in triplicate wells of a 6 well plate and incubated for 14 days with media changes every 3-4 days.

Figure 4. vBA-MSC suppression of T cell activation. (A) Suppression at decreasing ratios of PBMC to vBA-MSC. PBMC isolated from the blood of a single donor were labeled with carboxyfluorescein diacetate succinimidyl ester (CSFE). vBA-MSC were allowed to adhere 2 hours in 96 well plates before washing and adding 4x10^5 PBMC. In some experiments IFN-γ (100 ng/ml) was added 18-24 hours before adding PBMC. T cells were stimulated for 4 days with PHA. Cells were recovered from the plates and analyzed by flow cytometry after labeling with anti-CD3-PE antibodies. The percentage of activated T cells is plotted. (B) Representative flow plots for PBMCs alone, without and with PHA activation as well as PBMC and MSC after PHA activation are shown. Each data point represents the mean of 3 different experiments with 3 different donors (DD1, DD2 and DD3). Error bars represent the standard deviation. P>0.05 for comparisons at all PBMC:vBA-MSC ratios +/- IFN-γ.

Figure 5. Comparison of vBA-MSC to BM-MSC. (A) Surface marker expression of passage 3 cells was characterized by flow cytometry. The different sources of MSC were: deceased donor vBA-MSC (DD vBA-MSC); deceased donor vertebral body bone marrow-derived MSC (DD BM-MSC); living donor aspirated BM MSC (LD BM-MSC); and living donor aspirated BM MSC obtained from a commercial sources at passage 2 (LD Ex BM-MSC). The percentage of cells within the total population after gating out debris is shown. There were no differences in surface marker expression between cell types. (B-D) Comparison of

population doubling times (PDT) from passages 2 to 3 (B), 3 to 4 (C) and 4 to 5 (D). LD Ex BM-MSC grew significantly (*, P<0.05) slower between passage 2 and 3 than either vBA-MSC and LD BM-MSC. No difference in PDT was observed in the subsequent 2 passages. (**E**) CFU-F assays were performed as described in Figure 3 for passaged cells. Formation of CFU-F was significantly lower (*, P<0.05) for passage 2 LD Ex BM-MSC compared to the other three sources of MSC, also at passage 2. Each bar represents the mean $\pm$ sd from the 3 donors for each MSC source. The specific donors were: LD BM-MSC (donors LD1, LD2 and LD3); LD Ex BM-MSC (donors LD4, LD5 and LD6); vBM-MSC and vBA-MSC (donors DD1, DD2 and DD3). Donor characteristics are listed in Table 1.

Figure 6. Trilineage differentiation of vBA-MSC and MSC isolated from deceased donor vertebral body BM and BM aspirated from the iliac crests of living donors. Cells were cultured and induced to undergo differentiation for each cell type as described in Figure 2. There were no qualitative differences in either adipogenic, chondrogenic and osteogenic potential of passage 3 cells from any of the four sources. Images are representative from experiments with the 3 different donors for each source of MSC. Magnification is indicated on each image.

Figure 7. Cumulative population growth of vBA-MSC from 3 different donors. vBA-MSC obtained from digested fragments (5 g) of VBs from 3 donors (DD5, DD6 and DD7) were isolated and expanded to passage 1 to form a master cell bank. A portion of the passage 1 vBA-MSC from each donor was expanded to passage 9. (A) Observed and potential cumulative growth yields at each passage of vBA-MSC from 3 donors. (B) Cumulative vBA-MSC population doublings at passages 0-9. Population doublings (PD) were calculated based on initial numbers of cells plated and the number recovered after each plate reached 80% confluency before replating the cells and was used to determine the theoretical total cell yield after each passage. Theoretical total yields at passages 2-9 were obtained by exponentiating (base 2) the PD calculated for each passage and multiplying by the cumulative cell number from each preceding passage. Each donor vBA-MSC was plated in triplicate for each passage. The coefficient of variation (CV) between cell numbers obtained from each well was <15%.
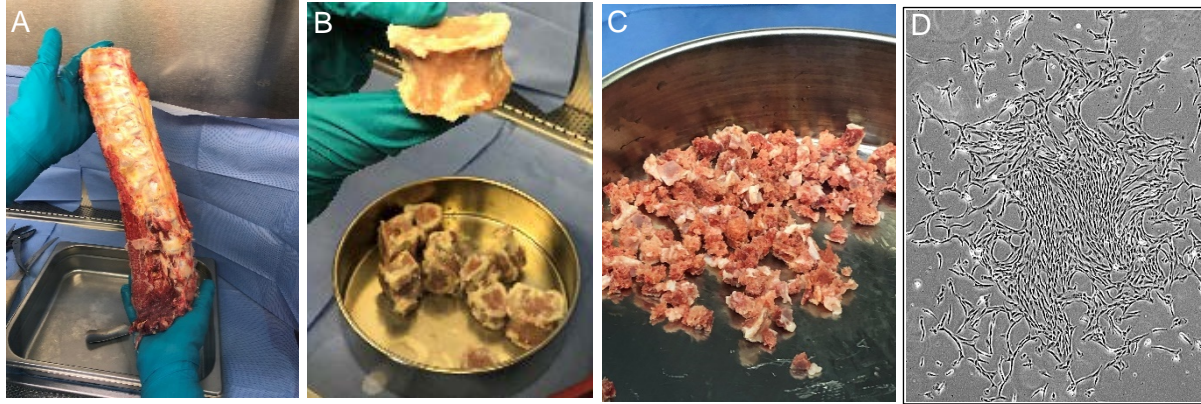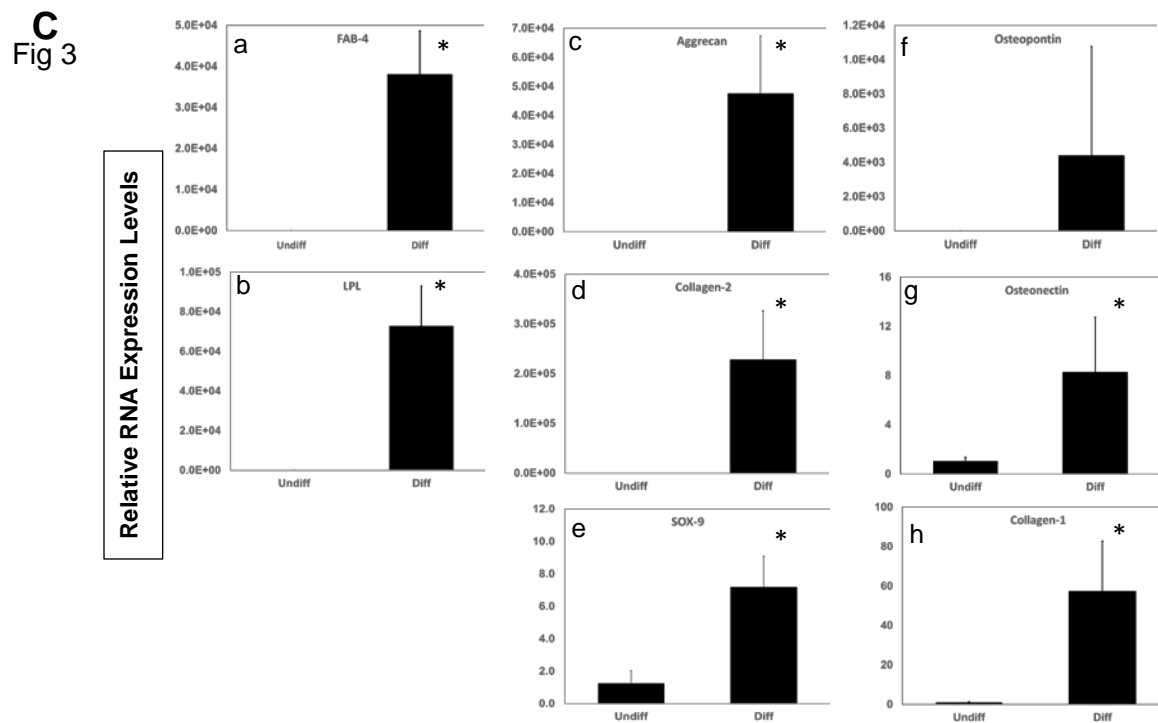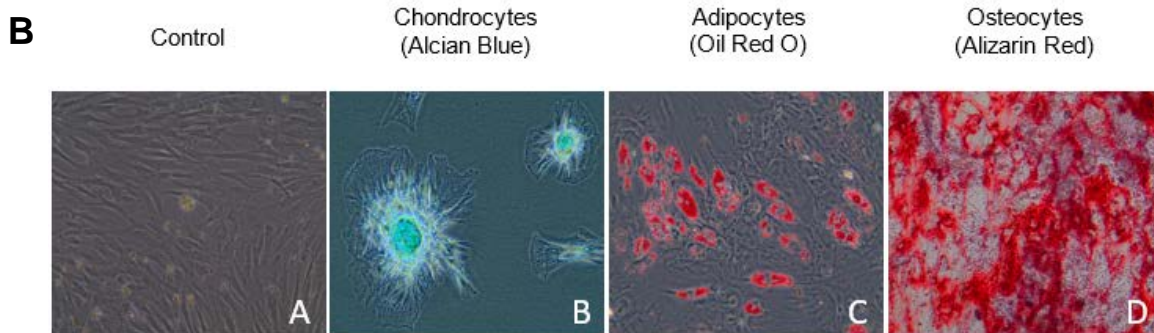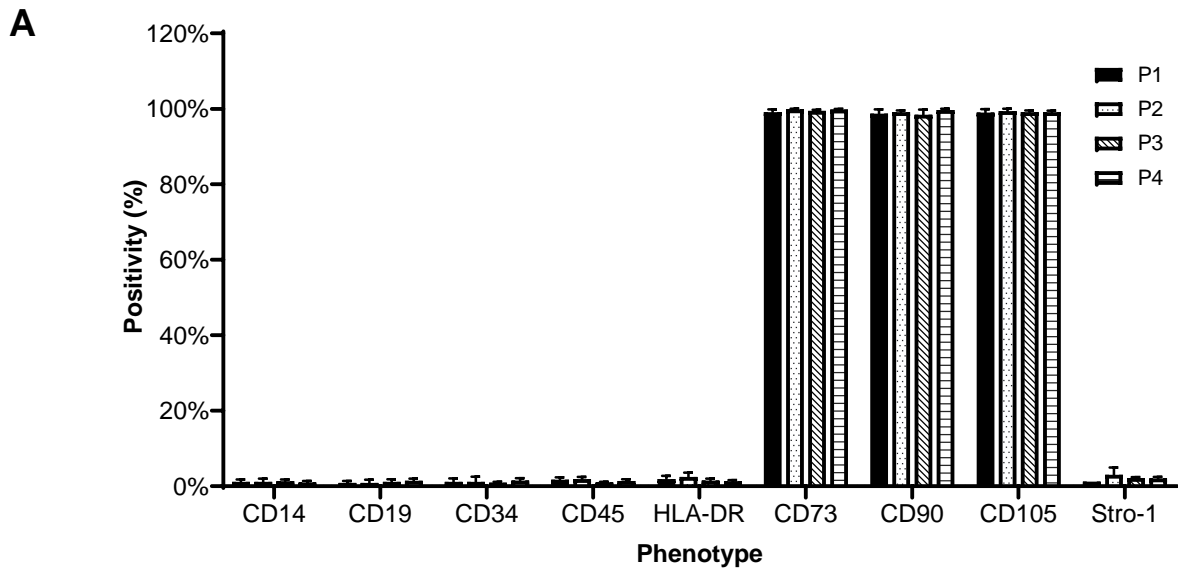
Fig 1

Fig 2

A

B

C

Fig 3

Fig 4

Fig 5

Fig 6

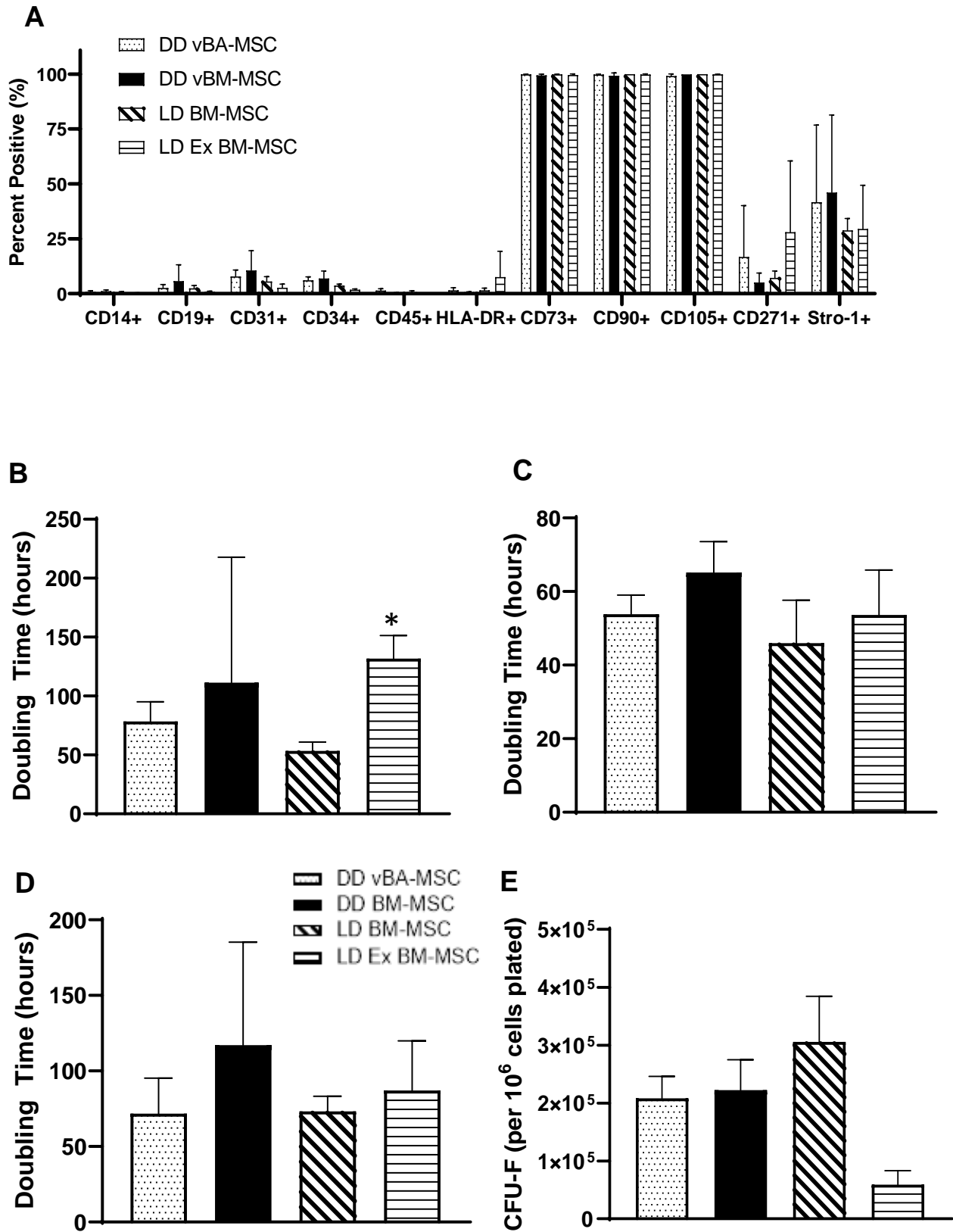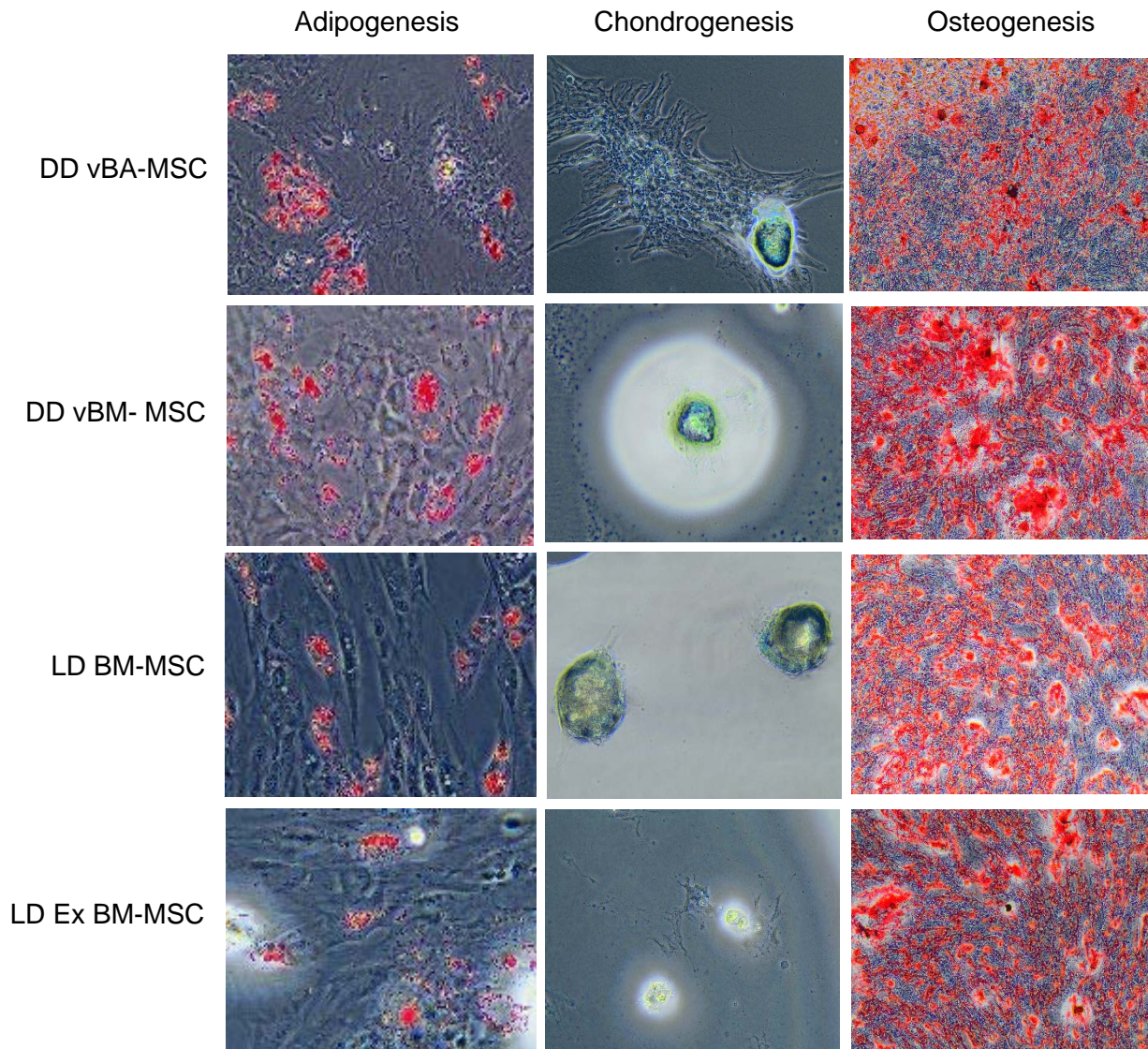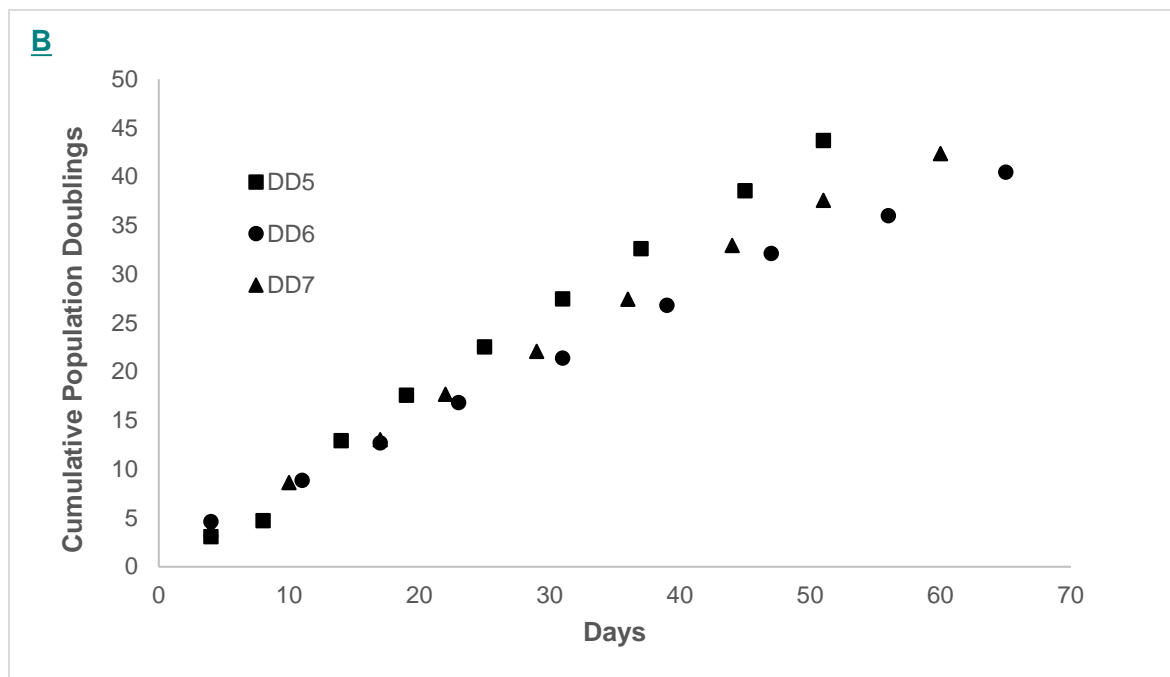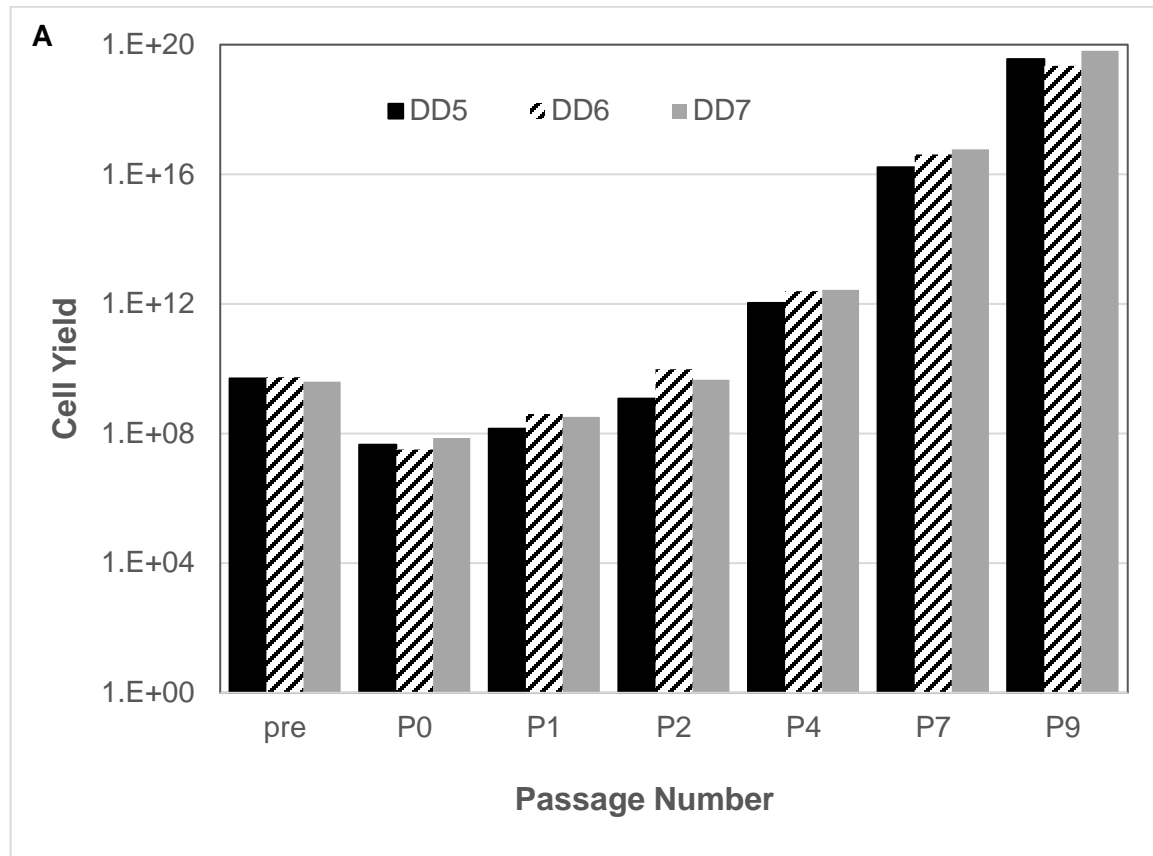|	Adipogenesis	Chondrogenesis	Osteogenesis
DD vBA-MSC			
DD vBM- MSC			
LD BM-MSC			
LD Ex BM-MSC			
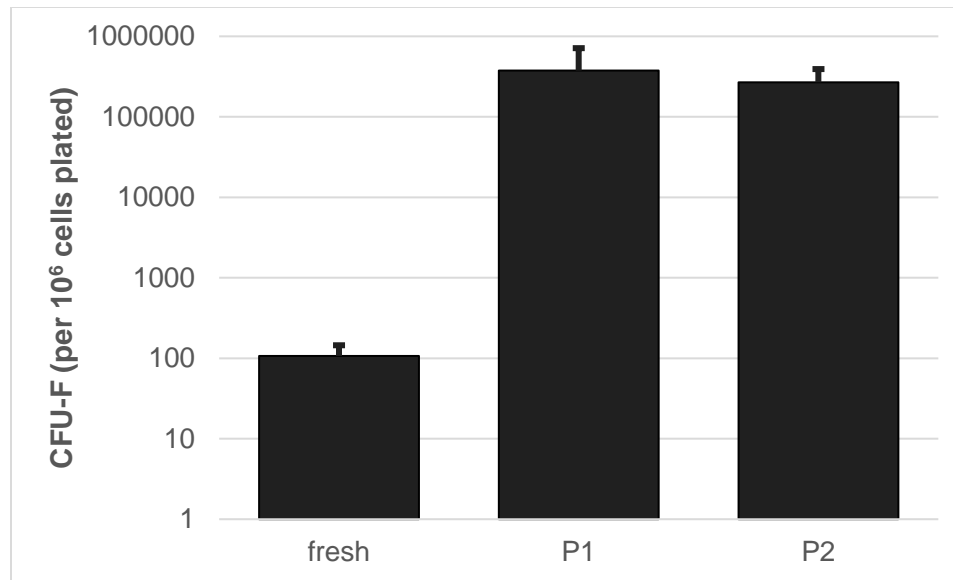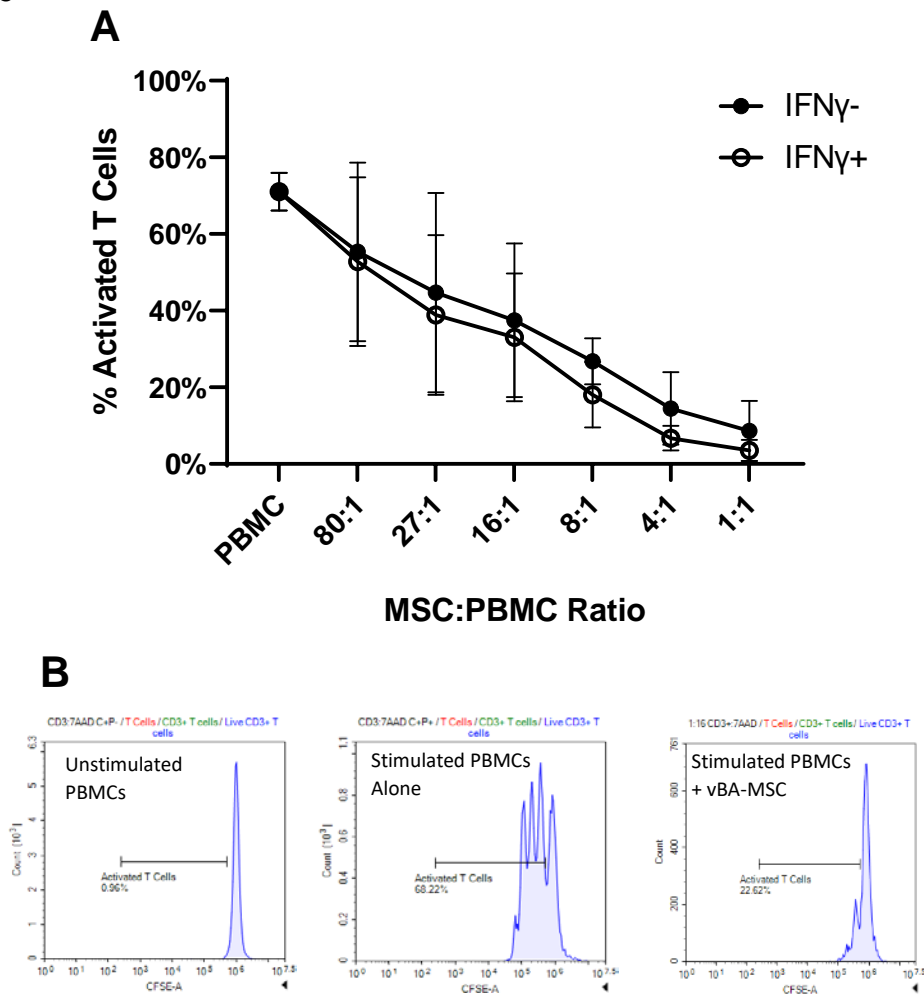
Fig 7

Supplemental data

Supplemental Table S1. Description of antibodies and dyes used

Antibody	Fluorophore	Clone	Isotype	Source
CD3	PE	UCHT1	IgG1-PE	BD
CD14	PE	MφP9	IgG2b-PE	BD
CD19	PE	4G7	IgG1-PE	BD
CD31	PE	MBC78.2	IgG1-PE	BD
CD34	PE	8G12	IgG1-PE	BD
CD45	APC	F10-89-4	IgG2a-APC	Caprico
HLA-DR	APC	L243	IgG2a-APC	Caprico
CD73	PeCy7	TY/11.8	IgG1-PeCy7	Biolegend
CD90	FITC	F15-42-1	IgG1-FITC	Caprico
CD105	APC	43A3	IgG1-APC	Biolegend
Stro-1	APC	STRO-1	IgM-APC	ThermoFisher
7AAD[1]	--	--	--	Invitrogen

[1]Abbreviations: 7-AAD, 7-aminoactinomycin; PE, phycoerythrin; APC, allophycocyanin; PeCy7, phycoerythrin-cyanin 7; FITC, fluorescein isothiocyanate.

Supplemental Table S2. Description of primers used

Gene	Primer Sequence	Reference
Fatty acid binding protein 4 (FABP4)	F: 5'-ATACTGGGCCAGGAATTTGAC-3' R: 5'-CGCATTCCACCACCAGTTTA-3'	1
Lipoprotein lipase (LPL)	F: 5'-CTTGGAGATGTGGACCAGC-3' R: 5'-GTGCCATACAGAGAAATCTC-3'	2
Osteonectin (ON)	F: 5'-CCCATTGGCGAGTTTGAGAA-3' R: 5'-GATGTATTTGCAAGGCCCGA-3'	2
Osteopontin (OPN)	F: 5'-ACTGATTTTCCCACGGAC-3' R: 5'-ATGGCTGTGGAATTCACG-3'	2
Aggrecan (ACAN)	F: 5'-TCGAGGACAGCGAGGCC-3' R: 5'-TCGAGGGTGTAGCGTGTAGAGA-3'	1
Collagen Type-1	F: 5'-CCGCCGCTTCACCTACAGC-3' R: 5'-TTTTGTATTCAATCACTGTCTTGCC-3'	1
Collagen Type-2	F: 5'-GGCAATAGCAGGTTCACGTACA-3' R: 5'-CGATAACAGTCTTGCCCCACTT-3'	1
GAPDH	F: 5'-ATGGGGAAGGTGAAGGTCG-3' R: 5'-TAAAAGCAGCCCTGGTGACC-3'	1
OCT4	F: 5'-ACATCAAAGCTCTGCAGAAAGAACT-3' R: 5'-CTGAATACCTTCCCAAATAGAACCC-3'	1
SOX9	F: 5'-CACACAGCTCACTCGACCTTG-3' R: 5'-TTCGGTTATTTTTAGGATCATCTCG-3'	1

1. Indrawattana et al. Growth factor combination for chondrogenic induction from human mesenchymal stem cell. Biochem Biophys Res Commun. 2004 Jul 30;320(3):914-9.

2. Patel et al. Mesenchymal stem cell population isolated from the subepithelial layer of umbilical cord tissue. Cell Transplant. 2013;22(3):513-9.
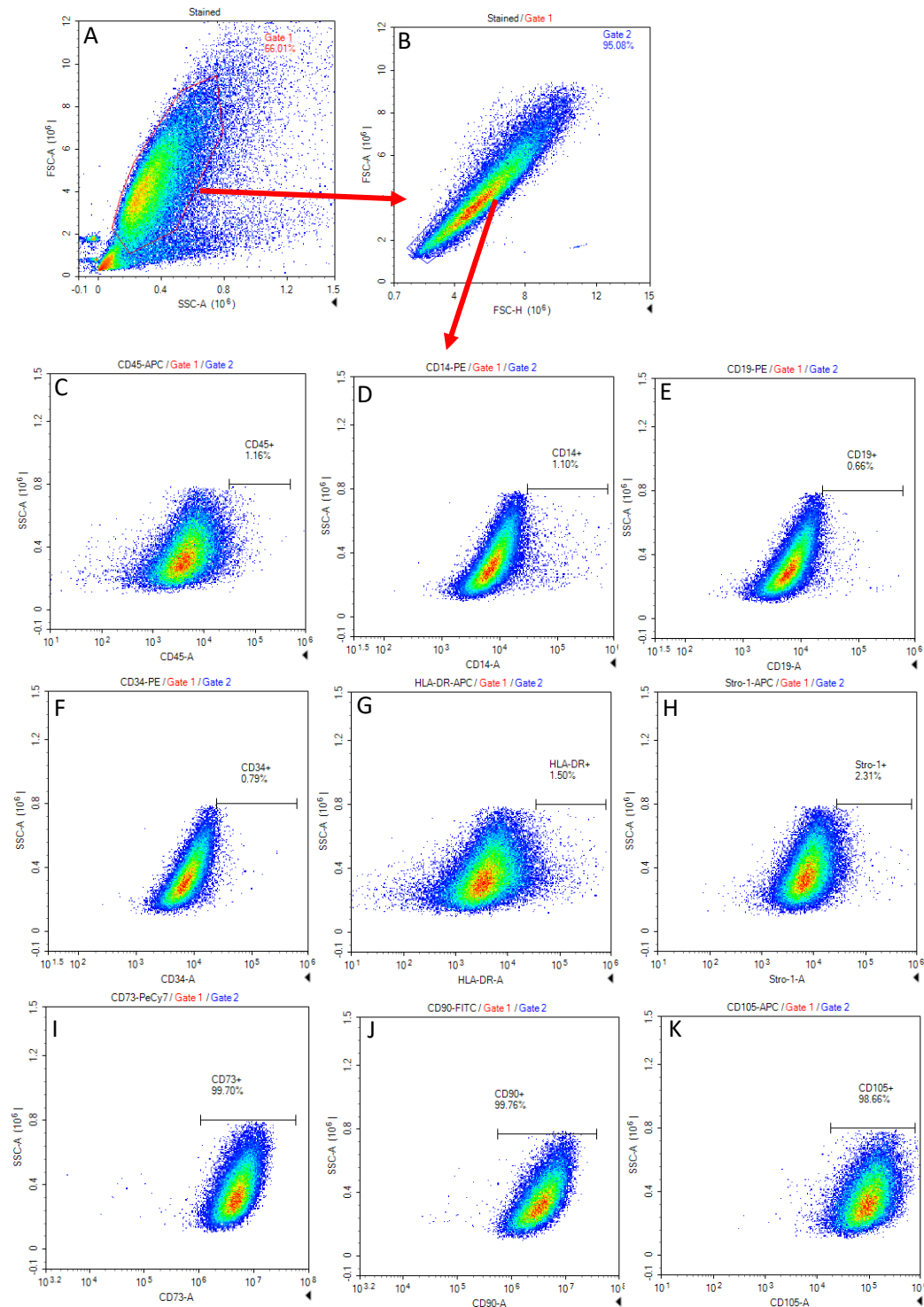
Supplemental Figure S1

Figure S1. Representative flow cytometry dot plots demonstrating the gating strategy used to identify passaged MSC by size based on forward and side scatter (A) and then single cells by forward scatter area over height (B). Single cells were then analyzed for the indicated cell surface epitopes (H-K) after setting gates based on a negative signal using

fluorescently conjugated isotype control antibodies (supplemental table S2).**REFERENCES**

1. Lipsitz, Y.Y., et al., *A roadmap for cost-of-goods planning to guide economic production of cell therapy products.* Cytotherapy, 2017. **19**(12): p. 1383-1391.
2. Olsen, T.R., et al., *Peak MSC-Are We There Yet?* Front Med (Lausanne), 2018. **5**: p. 178.
3. Pereira Chilimia, T.D., F. Moncaugeig, and S.S. Farid, *Impact of allogeneic stem cell manufacturing decisions on cost of goods, process robustness and reimbursement.* Biochemical Engineering Journal, 2018. **137**: p. 132-151.
4. Simaria, A.S., et al., *Allogeneic cell therapy bioprocess economics and optimization: single-use cell expansion technologies.* Biotechnol Bioeng, 2014. **111**(1): p. 69-83.
5. Harrison, R.P., N. Medcalf, and Q.A. Rafiq, *Cell therapy-processing economics: small-scale microfactories as a stepping stone toward large-scale macrofactories.* Regen Med, 2018. **13**(2): p. 159-173.
6. Mizukami, A., et al., *Technologies for large-scale umbilical cord-derived MSC expansion: Experimental performance and cost of goods analysis.* Biochemical Engineering Journal, 2018. **135**: p. 36-48.
7. Pittenger, M.F., et al., *Multilineage potential of adult human mesenchymal stem cells.* Science, 1999. **284**(5411): p. 143-7.
8. Chilima, T.D.P., T. Bovy, and S.S. Farid, *Designing the optimal manufacturing strategy for an adherent allogeneic cell therapy.* BioProcess International, 2016. **14**(9): p. 24-32.
9. Heathman, T.R., et al., *Characterization of human mesenchymal stem cells from multiple donors and the implications for large scale bioprocess development.* Biochemical Engineering Journal, 2016. **108**: p. 14-23.
10. Lechanteur, C., et al., *Large-scale clinical expansion of mesenchymal stem cells in the GMP-compliant, closed automated Quantum(R) cell expansion system: Comparison with expansion in traditional T-flasks.* Stem Cell Research & Therapy, 2014. **4**(8): p. 1-11.
11. Wuchter, P., et al., *Standardization of Good Manufacturing Practice-compliant production of bone marrow-derived human mesenchymal stromal cells for immunotherapeutic applications.* Cytotherapy, 2015. **17**(2): p. 128-39.
12. Chinnadurai, R., et al., *Immune dysfunctionality of replicative senescent mesenchymal stromal cells is corrected by IFNgamma priming.* Blood Adv, 2017. **1**(11): p. 628-643.
13. Mendicino, M., et al., *MSC-based product characterization for clinical trials: an FDA perspective.* Cell Stem Cell, 2014. **14**(2): p. 141-5.
14. Lockhart, R.A., J.A. Aronowitz, and S. Dos-Anjos Vilaboa, *Use of Freshly Isolated Human Adipose Stromal Cells for Clinical Applications.* Aesthet Surg J, 2017. **37**(suppl_3): p. S4-S8.
15. Dykstra, J.A., et al., *Concise Review: Fat and Furious: Harnessing the Full Potential of Adipose-Derived Stromal Vascular Fraction.* Stem Cells Transl Med, 2017. **6**(4): p. 1096-1108.
16. Donnenberg, A.D., et al., *Clinical implementation of a procedure to prepare bone marrow cells from cadaveric vertebral bodies.* Regen Med, 2011. **6**(6): p. 701-6.
17. Ahrens, N., et al., *Mesenchymal stem cell content of human vertebral bone marrow.* Transplantation, 2004. **78**(6): p. 925-9.
18. Cox, G., et al., *High abundance of CD271(+) multipotential stromal cells (MSCs) in intramedullary cavities of long bones.* Bone, 2012. **50**(2): p. 510-7.
19. Rybka, W.B., et al., *Hematopoietic progenitor cell content of vertebral body marrow used for combined solid organ and bone marrow transplantation.* Transplantation, 1995. **59**(6): p. 871-4.

20. Soderdahl, G., et al., *Cadaveric bone marrow and spleen cells for transplantation.* Bone Marrow Transplant, 1998. **21**(1): p. 79-84.

21. Blashki, D., et al., *Mesenchymal stem cells from cortical bone demonstrate increased clonal incidence, potency, and developmental capacity compared to their bone marrow-derived counterparts.* J Tissue Eng, 2016. **7**: p. 2041731416661196.

22. Siclari, V.A., et al., *Mesenchymal progenitors residing close to the bone surface are functionally distinct from those in the central bone marrow.* Bone, 2013. **53**(2): p. 575-86.

23. Yusop, N., et al., *Isolation and Characterisation of Mesenchymal Stem Cells from Rat Bone Marrow and the Endosteal Niche: A Comparative Study.* Stem Cells Int, 2018. **2018**: p. 6869128.

24. Jones, E., et al., *Large-scale extraction and characterization of CD271+ multipotential stromal cells from trabecular bone in health and osteoarthritis: implications for bone regeneration strategies based on uncultured or minimally cultured multipotential stromal cells.* Arthritis Rheum, 2010. **62**(7): p. 1944-54.

25. Gorantla, V.S., et al., *Development and validation of a procedure to isolate viable bone marrow cells from the vertebrae of cadaveric organ donors for composite organ grafting.* Cytotherapy, 2012. **14**(1): p. 104-13.

26. Li, M., et al., *Therapeutic Delivery Specifications Identified Through Compartmental Analysis of a Mesenchymal Stromal Cell-Immune Reaction.* Sci Rep, 2018. **8**(1): p. 6816.

27. Quah, B.J., H.S. Warren, and C.R. Parish, *Monitoring lymphocyte proliferation in vitro and in vivo with the intracellular fluorescent dye carboxyfluorescein diacetate succinimidyl ester.* Nat Protoc, 2007. **2**(9): p. 2049-56.

28. Dominici, M., et al., *Minimal criteria for defining multipotent mesenchymal stromal cells. The International Society for Cellular Therapy position statement.* Cytotherapy, 2006. **8**(4): p. 315-7.

29. Gronthos, S., et al., *Molecular and cellular characterisation of highly purified stromal stem cells derived from human bone marrow.* J Cell Sci, 2003. **116**(Pt 9): p. 1827-35.

30. Simmons, P.J. and B. Torok-Storb, *Identification of stromal cell precursors in human bone marrow by a novel monoclonal antibody, STRO-1.* Blood, 1991. **78**(1): p. 55-62.

31. Dennis, J.E., et al., *The STRO-1+ marrow cell population is multipotential.* Cells Tissues Organs, 2002. **170**(2-3): p. 73-82.

32. Bensidhoum, M., et al., *Homing of in vitro expanded Stro-1- or Stro-1+ human mesenchymal stem cells into the NOD/SCID mouse and their role in supporting human CD34 cell engraftment.* Blood, 2004. **103**(9): p. 3313-9.

33. Galipeau, J., et al., *International Society for Cellular Therapy perspective on immune functional assays for mesenchymal stromal cells as potency release criterion for advanced phase clinical trials.* Cytotherapy, 2016. **18**(2): p. 151-9.

34. Squillaro, T., G. Peluso, and U. Galderisi, *Clinical Trials With Mesenchymal Stem Cells: An Update.* Cell Transplant, 2016. **25**(5): p. 829-48.

35. Eom, Y.W., et al., *The role of growth factors in maintenance of stemness in bone marrow-derived mesenchymal stem cells.* Biochem Biophys Res Commun, 2014. **445**(1): p. 16-22.

36. Galipeau, J. and L. Sensebe, *Mesenchymal Stromal Cells: Clinical Challenges and Therapeutic Opportunities.* Cell Stem Cell, 2018. **22**(6): p. 824-833.

37. Jossen, V., et al., *Manufacturing human mesenchymal stem cells at clinical scale: process and regulatory challenges.* Appl Microbiol Biotechnol, 2018. **102**(9): p. 3981-3994.

38. Banfi, A., et al., *Replicative aging and gene expression in long-term cultures of human bone marrow stromal cells.* Tissue Eng, 2002. **8**(6): p. 901-10.

39. Baxter, M.A., et al., *Study of telomere length reveals rapid aging of human marrow stromal cells following in vitro expansion.* Stem Cells, 2004. **22**(5): p. 675-82.

40. Bork, S., et al., *DNA methylation pattern changes upon long-term culture and aging of human mesenchymal stromal cells.* Aging Cell, 2010. **9**(1): p. 54-63.

41. Bruder, S.P., N. Jaiswal, and S.E. Haynesworth, *Growth kinetics, self-renewal, and the osteogenic potential of purified human mesenchymal stem cells during extensive subcultivation and following cryopreservation.* J Cell Biochem, 1997. **64**(2): p. 278-94.

42. Digirolamo, C.M., et al., *Propagation and senescence of human marrow stromal cells in culture: a simple colony-forming assay identifies samples with the greatest potential to propagate and differentiate.* Br J Haematol, 1999. **107**(2): p. 275-81.

43. Muraglia, A., R. Cancedda, and R. Quarto, *Clonal mesenchymal progenitors from human bone marrow differentiate in vitro according to a hierarchical model.* J Cell Sci, 2000. **113 (Pt 7)**: p. 1161-6.

44. Redaelli, S., et al., *From cytogenomic to epigenomic profiles: monitoring the biologic behavior of in vitro cultured human bone marrow mesenchymal stem cells.* Stem Cell Res Ther, 2012. **3**(6): p. 47.

45. Moravcikova, E., et al., *Proteomic Profiling of Native Unpassaged and Culture-Expanded Mesenchymal Stromal Cells (MSC).* Cytometry A, 2018. **93**(9): p. 894-904.

46. Bara, J.J., et al., *Concise review: Bone marrow-derived mesenchymal stem cells change phenotype following in vitro culture: implications for basic research and the clinic.* Stem Cells, 2014. **32**(7): p. 1713-23.

47. Choi, Y.H. and J.K. Kim, *Dissecting Cellular Heterogeneity Using Single-Cell RNA Sequencing.* Mol Cells, 2019. **42**(3): p. 189-199.

48. Hwang, B., J.H. Lee, and D. Bang, *Single-cell RNA sequencing technologies and bioinformatics pipelines.* Exp Mol Med, 2018. **50**(8): p. 96.

49. Wu, L.W., et al., *Donor age negatively affects the immunoregulatory properties of both adipose and bone marrow derived mesenchymal stem cells.* Transpl Immunol, 2014. **30**(4): p. 122-7.

50. Barreto-Duran, E., et al., *Impact of donor characteristics on the quality of bone marrow as a source of mesenchymal stromal cells.* Am J Stem Cells, 2018. **7**(5): p. 114-120.

51. Beane, O.S., et al., *Impact of aging on the regenerative properties of bone marrow-, muscle-, and adipose-derived mesenchymal stem/stromal cells.* PLoS One, 2014. **9**(12): p. e115963.

52. Katsara, O., et al., *Effects of donor age, gender, and in vitro cellular aging on the phenotypic, functional, and molecular characteristics of mouse bone marrow-derived mesenchymal stem cells.* Stem Cells Dev, 2011. **20**(9): p. 1549-61.

53. Baker, N., L.B. Boyette, and R.S. Tuan, *Characterization of bone marrow-derived mesenchymal stem cells in aging.* Bone, 2015. **70**: p. 37-47.

54. Schimke, M.M., S. Marozin, and G. Lepperdinger, *Patient-Specific Age: The Other Side of the Coin in Advanced Mesenchymal Stem Cell Therapy.* Front Physiol, 2015. **6**: p. 362.

55. Charif, N., et al., *Aging of bone marrow mesenchymal stromal/stem cells: Implications on autologous regenerative medicine.* Biomed Mater Eng, 2017. **28**(s1): p. S57-S63.

56. Arshad, A., B. Anderson, and A. Sharif, *Comparison of organ donation and transplantation rates between opt-out and opt-in systems.* Kidney Int, 2019. **95**(6): p. 1453-1460.